Joint Simple Blind IQ Imbalance Compensation and Adaptive Equalization for 16-QAM Optical Communications

Trung Hien Nguyen, Pascal Scalart, Michel Joindot, Mathilde Gay, Laurent Bramerie, Christophe Peucheret, Arnaud Carer, Jean-Claude Simon, Olivier Sentieys

▶ **To cite this version:**

Trung Hien Nguyen, Pascal Scalart, Michel Joindot, Mathilde Gay, Laurent Bramerie, et al.. Joint Simple Blind IQ Imbalance Compensation and Adaptive Equalization for 16-QAM Optical Communications. IEEE International Conference on Communications, Jun 2015, Londres, United Kingdom. pp.4913 - 4918, 10.1109/ICC.2015.7249101 . hal-01162391

HAL Id: hal-01162391
https://hal.science/hal-01162391

Submitted on 10 Jun 2015

HAL is a multi-disciplinary open access archive for the deposit and dissemination of scientific research documents, whether they are published or not. The documents may come from teaching and research institutions in France or abroad, or from public or private research centers.

L'archive ouverte pluridisciplinaire **HAL**, est destinée au dépôt et à la diffusion de documents scientifiques de niveau recherche, publiés ou non, émanant des établissements d'enseignement et de recherche français ou étrangers, des laboratoires publics ou privés.

Joint Simple Blind IQ Imbalance Compensation and Adaptive Equalization for 16-QAM Optical Communications

Trung-Hien Nguyen[1], Pascal Scalart[2], Michel Joindot[1], Mathilde Gay[1], Laurent Bramerie[1], Christophe Peucheret[1], Arnaud Carer[2], Jean–Claude Simon[1] and Olivier Sentieys[2]
[1] FOTON Laboratory, CNRS, University of Rennes 1, ENSSAT, F-22305 Lannion, France
[2] INRIA / IRISA, Campus Beaulieu, 35000 Rennes, France
trung-hien.nguyen@enssat.fr

***Abstract*— We present a novel simple blind adaptive compensation method for in-phase/quadrature (IQ) imbalance in *m*-ary quadrature amplitude modulation (*m*–QAM) coherent optical fiber communication systems. IQ-imbalance compensation is integrated into butterfly-structured finite impulse response (FIR) filters, resulting in a significant computational effort reduction in comparison to conventional methods. A reduction in hardware complexity by a factor of about 3 is achieved by the proposed joint method. The proposed structure is experimentally validated with a 40–Gbit/s 16-QAM signal. A 7-dB power penalty reduction is experimentally achieved at a bit error rate (BER) of 10^{-3} in the presence of a 10° phase imbalance, confirming the effectiveness of the proposed algorithm. The equalization capability remains even in the presence of group velocity dispersion along the link, which is numerically confirmed with optical fiber transmission up to 1200 km and 20° phase imbalance.**

***Keywords*— Coherent optical fiber communications; m-QAM; IQ imbalance; adaptive filter**

I. INTRODUCTION

Coherent detection of *m*–ary quadrature amplitude modulation (*m*-QAM) signals and digital signal processing (DSP) are promising solutions for the implementation of next generation optical transmission systems [1]. However, as the number of modulation levels increases, the sensitivity to system imperfections such as phase noise of the transmitter and the local oscillator lasers or fiber nonlinearities is exacerbated. Moreover, the amplitude and phase imbalances between the in-phase (I) and quadrature (Q) channels in the transmitter (Tx) and the front-end of the receiver (Rx), which is often referred to as IQ imbalance, is also troublesome if not compensated. IQ imbalance may be introduced by either incorrect bias settings of the modulators in transmitters or hardware implementation imperfections in 90° optical hybrids, balanced photodiodes, or trans-impedance amplifiers in receiver front-ends.

Some effort has been dedicated to the compensation of IQ imbalance with the help of DSP. IQ imbalance causing inter-carrier interference (ICI) due to imperfect image rejection in multicarrier direct-detection systems has been analytically and numerically investigated [2]. In multicarrier coherent-detection systems, several frequency domain compensation methods for IQ imbalance have been reported, both for wireless and optical transmission. Those include the joint Tx and Rx IQ imbalance compensation [3, 4], the pilot-assisted method [5], the use of a novel training symbol structure [6], or the joint compensation of phase noise and IQ imbalance [7]. For single carrier optical coherent detection systems, some work exploiting time-domain compensation has been numerically and experimentally carried out. More specifically, IQ imbalance has been corrected in optical coherent quadrature phase-shift keying (QPSK) systems by applying different methods such as the Gram-Schmidt orthogonalization procedure (GSOP) [8], the ellipse correction method (EC) [9], and IQ compensations based on the constant modulus algorithm (CMA) [10] or the statistical properties of received signals [11].

In high bit rate transmission, inter-symbol interference (ISI) is unavoidable due to bandwidth limitations at the Tx/Rx or linear and nonlinear propagation effects during optical fiber transmission. An equalizer stage is therefore required to cancel the ISI. However, the equalization stage alone cannot compensate for IQ imbalance [12]. The idea to combine IQ imbalance compensation with the equalization stage, which customarily includes polarization demultiplexing, chromatic dispersion compensation and timing recovery, was suggested in [12] as a computational simplification. The proposed solution was a modified version of the conventional adaptive finite-impulse-response (FIR) filters in a butterfly configuration structure [12]. However, the required number of FIR filter coefficients-sets in this configuration is 2 times larger than in the conventional one, thereby significantly increasing the implementation complexity.

In this paper, we propose a novel simple blind adaptive IQ imbalance compensation based on a decision-directed least-mean-square (DD-LMS) algorithm integrated to a modified butterfly FIR filter configuration. This method is blind in the sense that no known training symbols are required [2]. Since only 2 FIR filter coefficients-sets are used, instead of 4 in the conventional configuration, the time for updating the

coefficients and the hardware resources (such as coefficient memories and number of look-up tables) in real time field-programmable gate array (FPGA) platforms is then reduced using this method. The method is validated using a 16-QAM signal in this work, however it can be applied to any single-carrier advanced modulation format, which is a desirable feature in the context of flexible optical transceivers [13]. In addition, carrier phase recovery is simultaneously achieved during the adaptive coefficients update, thanks to a digital phase-locked loop (DPLL) based on a second-order loop filter [14]. The performance of the proposed IQ imbalance compensation method is experimentally evaluated in terms of bit error rate (BER) measurements. A power penalty reduction of 7 dB is achieved at a BER of 10^{-3} for 10° phase imbalance, indicating the effectiveness of this algorithm. Moreover, optical fiber transmission up to 1200 km and 20° phase imbalance are numerically studied in the presence of group velocity dispersion, demonstrating that the performance of the equalizer is not weakened by its combination with IQ imbalance compensation.

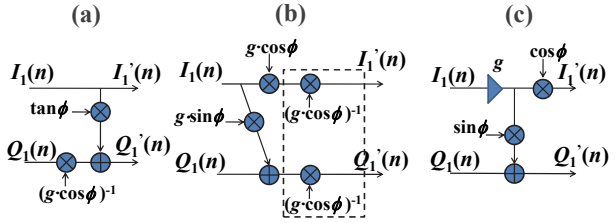

Fig. 1. (a) Conventional IQ imbalance compensator. (b) Equivalent configuration with a common factor at the outputs. (c) Simplified version of the IQ imbalance compensator.

II. Proposed Method for IQ Imbalance Compensation

Among the state-of-the-art of IQ imbalance compensation, the method proposed in [11] showed better performance compared to other methods for large phase imbalance values. This particular configuration is represented in Fig. 1(a), in which g and ϕ are the relative amplitude and phase imbalances, respectively. I_1 and Q_1 are the acquired input samples representing the in-phase and quadrature components of the signal, while I_1' and Q_1' denote the output samples of the IQ compensators. An equivalent structure can be implemented using trigonometric transformations, as shown in Fig. 1(b). A common multiplying factor $(g\cdot\cos\phi)^{-1}$ appears and acts as a constant gain for the two outputs. This factor can be removed to achieve the simplified scheme for IQ imbalance compensation shown in Fig. 1(c). It turns out that, in such a structure, the impacts of amplitude and phase imbalances can be compensated independently.

In high bit rate transmission, an equalizer stage is required to cancel ISI. The integration of the simplified IQ imbalance compensator of Fig. 1(c) to the equalizer is feasible with low complexity. The detailed integrated configuration and its proof-of-concept operation are studied in the following sections.

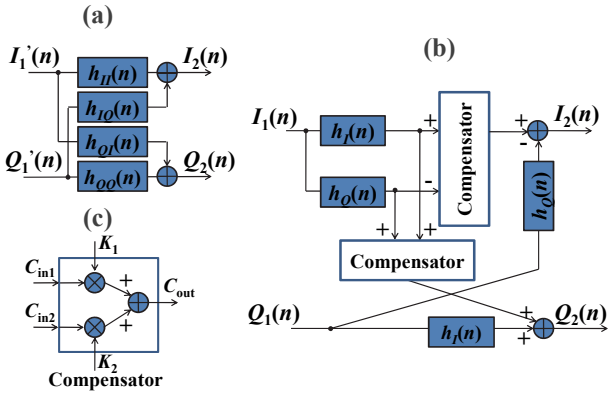

Fig. 2. (a) Conventional butterfly structured-FIR filters. (b) Proposed adaptive FIR filters. (c) Compensator structure.

III. Joint Equalization and IQ Imbalance Compensation

In our study, we compare the case where IQ imbalance compensation and equalization are performed successively (henceforth referred to as case 1) with our proposed method where both are performed simultaneously (case 2). In case 1, the structure of Fig. 1(a) is used to compensate for the IQ imbalance and is followed by conventional butterfly-structured FIR filters for equalization (Fig. 2(a)). This equalizer is defined by 4 FIR filter coefficients-sets (h_{II}, h_{IQ}, h_{QI} and h_{QQ}). The separate implementation of the IQ compensator could result in increased computational complexity. In particular, the calculation of the values of the amplitude and phase imbalance compensation coefficients requires some trigonometric and square-root operations [11], which can make the implementation in FPGAs more complex. To overcome this problem, we propose to integrate the IQ imbalance compensator of Fig. 1(c) into modified butterfly structured-FIR filters (case 2, represented in Fig. 2(b) with the compensator structures in Fig. 2(c)). The parameters C_{in1} and C_{in2} are the inputs of the compensator, whereas the output of the compensator is given by

$$C_{out} = K_1 \cdot C_{in1} + K_2 \cdot C_{in2}\,, \tag{1}$$

where the values of K_1 and K_2 are adaptively updated. The updating rules for the proposed IQ imbalance compensation are given by equations (2) and (3)

$$K_2(n+1) = K_2(n) + \mu_1 \cdot \Delta K_2(n)\,, \tag{2}$$

$$K_1(n+1) = \sqrt{1 - K_2^2(n+1)}\,, \tag{3}$$

in which μ_1 is a constant step-size parameter. ΔK_2 is calculated according to

$$\Delta K_2(n) = 2\Re\left\{e_1(n)\left[I_1(n)\otimes\left(-h_Q(n) + i\cdot h_I(n)\right) - \frac{K_2(n)}{K_1(n)} I_1(n)\otimes\left(h_I(n) + i\cdot h_Q(n)\right)\right]^*\right\} \tag{4}$$

where ⊗ and * denote the convolution and complex conjugate operators, respectively. Note that, when the asymptotic convergence is achieved, K_1 and K_2 can be deduced with respect to the phase imbalance ϕ as follows: $K_1 = \cos\phi$ and $K_2 = \sin\phi$. In practical implementations, the phase imbalance should be sufficiently well controlled so that its value remains in the range of $[-\pi/6, \pi/6]$. This range ensures that a positive value is obtained in the argument of the square root in (3). Because the amplitude imbalance could be compensated for by hardware implementations (such as the use of automatic gain controlled transimpedance amplifiers) and possibly partly by adaptive filters, it is neglected in this configuration.

The real-valued column vectors $I_1(n)$ and $Q_1(n)$ are the inputs to 2 ports of the filters, representing the real and imaginary part of the input signal samples, respectively. The corresponding outputs of the butterfly structured-FIR filters, $I_2(n)$ and $Q_2(n)$, are given by

$$I_2(n) = \left[K_1 \cdot h_I(n) - K_2 \cdot h_Q(n)\right]^T \cdot I_1(n) - \left[h_Q(n)\right]^T \cdot Q_1(n) \quad (5)$$

$$Q_2(n) = \left[K_2 \cdot h_I(n) + K_1 \cdot h_Q(n)\right]^T \cdot I_1(n) + \left[h_I(n)\right]^T \cdot Q_1(n), \quad (6)$$

where $[\cdot]^T$ denotes the transpose operator. The tap weights of the proposed structure are then updated according to

$$h_I(n+1) = h_I(n) + \mu_2 \cdot \Re\left\{e_1(n) \cdot e^{i\cdot\hat{\theta}(n)} \cdot \left[K_1 \cdot I_1(n) + i \cdot \left(K_2 \cdot I_1(n) + Q_1(n)\right)\right]^*\right\} \quad (7)$$

$$h_Q(n+1) = h_Q(n) + \mu_2 \cdot \Re\left\{e_1(n) \cdot e^{i\cdot\hat{\theta}(n)} \cdot \left[\left(-K_2 \cdot I_1(n) - Q_1(n)\right) + i \cdot K_1 \cdot I_1(n)\right]^*\right\} \quad (8)$$

where μ_2 is another step-size parameter and $\hat{\theta}(n)$ is the carrier phase estimation obtained from the DPLL, as described in the following section. $\Re$ denotes the real part operator and $i = \sqrt{-1}$ is the imaginary unit.

The error after direct decision, $e_1(n)$, is calculated according to equation (9)

$$e_1(n) = d(n) - \left[I_2(n) + i \cdot Q_2(n)\right] \cdot e^{-i\cdot\hat{\theta}(n)}, \quad (9)$$

where $d(n)$ represents the direct-decision symbol. The filter coefficients are updated in order to minimize the mean square error (MSE), $E(|e_1^2(n)|)$, after decision.

The proposed IQ imbalance compensator can be implemented using 4 multiplications and 2 additions, which adds a small complexity compared to case 1 (2 multiplications and 1 addition only in Fig. 1(a)). However, as far as the equalization stage is concerned, case 2 brings simplification compared to case 1: only 2 FIR filter coefficients-sets ($h_I(n)$ and $h_Q(n)$) are indeed required. Note that our modified FIR filters can integrate the IQ imbalance compensator because their updating rules both rely on LMS algorithms [16]. While our method is fully adaptive, the coefficients K_1 and K_2 estimated from the first processed block of samples can be applied without change to the following blocks to further reduce the computational effort in case of slowly varying imbalance values. The adaptive estimation of the imbalance value can be reactivated after an amount of time if necessary.

The hardware complexities of case 1 and case 2 as well as another recently reported method providing IQ imbalance compensation and equalization [12] are summarized in Table I. In this comparison, it is assumed that all equalizer structures have to compensate for the same channel impairments and can therefore be described by the same number of coefficients, N, for each FIR filter. Table I shows that the hardware complexity of case 2 remains nearly similar to that of case 1. Moreover, the total number of operators (adders and multipliers) required in both cases is reduced by a factor 3 in comparison to the one required in the method of [12]. Finally, case 2 results in a smaller computational effort than case 1 thanks to the reduction by a factor 2 of the coefficients-sets number.

TABLE I. HARDWARE COMPLEXITY AND COMPUTATIONAL EFFORT FOR VARIOUS IQ IMBALANCE COMPENSATION METHODS.

Methods	***Multipliers***	***Adders***	***Coefficients-sets number***
Case 1	$12N + 2$	$4N + 1$	4
Case 2 (this work)	$14N$	$6N$	2
Method [12]	$32N$	$32N$	8

IV. EXPERIMENTAL SETUP

The impact of non-orthogonality between I and Q channels is experimentally investigated in an optical 16-QAM coherent system, as shown in Fig. 3(a). In order to allow a fair comparison between the aforementioned cases 1 and 2, the same laser is used at the transmitter and as local oscillator (LO) at the receiver. In this way, no carrier frequency offset compensation is required. The estimated linewidth of this optical source is about 100 kHz. At the transmitter, two 4-level pulse amplitude modulation (PAM) sequences are constituted from two pseudo-random binary sequences (PRBSs) with lengths of $2^{11}-1$ and $2^{13}-1$ bits, to generate the 10-GSymbol/s data streams applied to a dual drive IQ modulator. The symbol sequences are generated with an arbitrary waveform generator (AWG).

Fig. 3(b) represents the configuration of the dual drive IQ modulator, which consists of one Mach-Zehnder modulator (MZM) in each arm and a phase shifter to realize the required 90° phase difference between the two branches. The 4-PAM sequences applied to the I and Q inputs of the modulator are decorrelated through a 64-symbol delay. The IQ imbalance is adjusted by modifying the bias voltage controlling the phase difference between the two arms of the IQ modulator. The received power is adjusted by means of a variable optical attenuator (VOA). The signal is then boosted by an erbium-

doped fiber amplifier (EDFA) followed by a 3-nm optical bandpass filter (OBPF). At the receiver side, an optical 90° hybrid (DP-QPSK integrated receiver) mixes the 16-QAM signal and the LO.

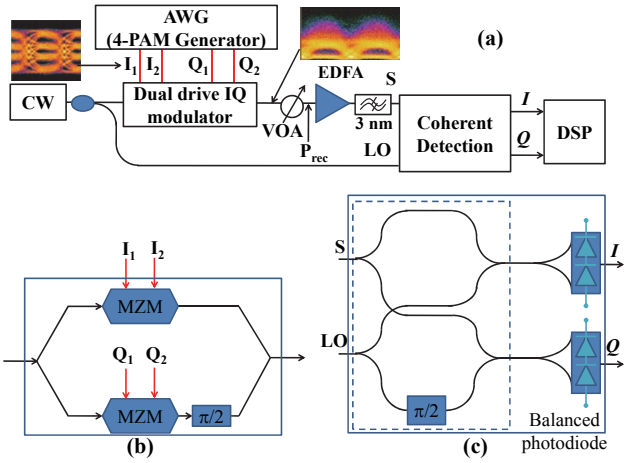

Fig. 3. (a) Experimental setup. (b) Dual drive IQ modulator structure. (c) Optical 90° hybrid structure.

The structure of this receiver is presented in Fig. 3(c). The signal and LO are first split. The split signal and LO are then cross-combined with proper phase shifts to produce two beating terms, namely *I* and *Q*. The 90° phase shift present in the lower branch of the splitting coupler for the LO results in the detection of the quadrature term, whereas the upper branch results in the detection of the in-phase term. The *I* and *Q* components are detected by balanced photodiodes and acquired by a real time oscilloscope with electrical bandwidth of 16 GHz at a sampling rate of 40 GS/s. After data acquisition, post-processing is performed offline using the Matlab environment.

To focus on the compensation of IQ imbalance in a 16–QAM system, polarization (de)multiplexing and chromatic dispersion effects due to transmission are ignored. Fig. 4(a) represents the schematic of the DSP blocks at the receiver side. In the first step of DSP, the proposed FIR filter operating at four times the symbol rate is applied to blocks of 200000 symbols. The received samples are then decimated to a symbol rate of 10 GS/s before being sent to the symbol-directed detector to calculate the mean square error. Moreover, a DPLL consisting of a second-order loop filter is employed to perform phase recovery [14]. Fig. 4(b) presents the structure of the second-order loop filter, in which α and β are the loop parameters. Based on the error achieved from the direct-decision, $e_1(n)$, and the decimated signal, $r_{dec}(n)$, the phase error [17] is calculated using equation (10)

$$e_2(n) = \Im\left\{ e_1^*(n) \cdot r_{dec}(n) \cdot \mathrm{e}^{-i\cdot\hat{\theta}(n)} \right\} \tag{10}$$

where $\Im$ denotes the imaginary part operator. Finally, the error is fed-back along with the carrier phase estimation to update the IQ compensators and FIR filters parameters. A comparison between the decoded and transmitted bit sequences is performed to determine the BER over 1 million samples. Fig. 4(c) shows an example of the estimated phase imbalance based on the proposed algorithm. The fast convergence of the estimated phase imbalance after processing of ~5000 symbols appears clearly.

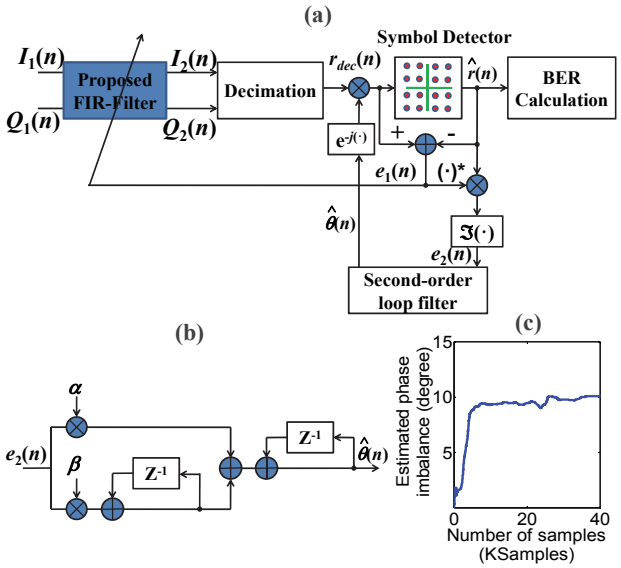

Fig. 4. (a) Schematic of DSP blocks for the received samples. (b) Second-order loop filter structure. (c) Convergence of the estimated phase imbalance.

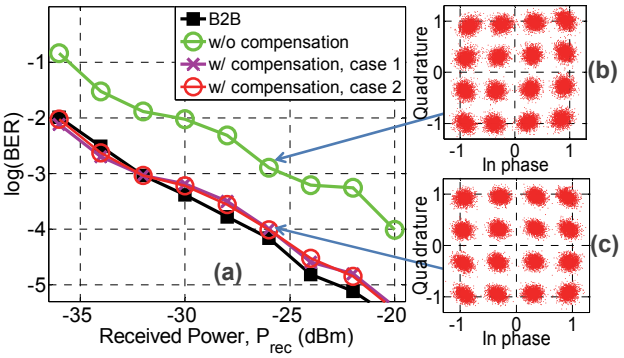

Fig. 5. BER versus received power for 10° phase imbalance.

V. Experimental Demonstration of IQ Imbalance Compensation

Fig. 5(a) presents the results of BER measurements as a function of received power in different cases. BER measurements without IQ imbalance (back-to-back curve, B2B) are plotted as a reference. Note that BER measurements are considered up to 10^{-5} due to the limitation of acquired symbols. This BER level is however sufficiently lower than the hard forward error correction (FEC) BER of 10^{-3} that enables to achieve an equivalent BER of 10^{-9}. In the presence of 10° phase imbalance, the BER is degraded, resulting in a power penalty of 7 dB at a BER of 10^{-3}. By using the proposed compensation (referred to as case 2), the BER curve matches the reference case again, leading to a 7 dB power penalty reduction. Experimental constellations obtained at –26 dBm

received power are presented in Fig. 5(b) and (c) for the distorted and the retrieved constellations, respectively, showing the effectiveness of the compensation. The proposed method is compared to the case where IQ imbalance compensation and equalization are performed separately (referred to as case 1). The excellent match between both BER curves demonstrates the effectiveness of the proposed algorithm, which exhibits a significantly reduced computational and hardware complexity without any performance loss.

Fig. 6 shows the power penalty at a BER of 10^{-3} with respect to the back-to-back case measured without and with compensation in case 1 and 2, respectively. Without compensation a power penalty of 12 dB is observed for a phase imbalance of 15°, indicating the high sensitivity to this kind of impairment. In contrast, a power penalty reduction of 11 dB is measured at 15° phase imbalance using either case 1 compensation or our simplified approach (case 2).

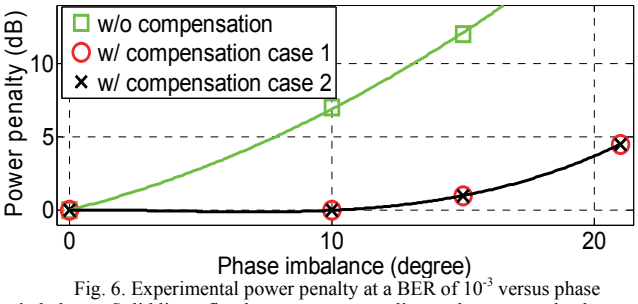

Fig. 6. Experimental power penalty at a BER of 10^{-3} versus phase imbalance. Solid lines: fitted curves corresponding to the measured values, represented with symbols.

VI. Numerical Demonstration of Chromatic Dispersion Compensation

Group-velocity dispersion (GVD) is a transmission impairment caused by different spectral components of a pulse propagating at different velocities over the optical fiber channel. This leads to pulse spreading and ISI if not compensated. We have so far validated the effectiveness of our IQ imbalance compensator in the absence of ISI. In this section, we numerically validate that the proposed joint IQ imbalance compensation and equalization does not affect the effectiveness of the equalizer in the presence of ISI induced by GVD.

To this aim, we simulate the transmission of a 10-Gbaud optical 16-QAM signal presenting 20° phase imbalance in the telecommunication wavelength window around 1550 nm. This signal is evaluated after the propagation over 1200 km standard single mode fiber (SSMF), with a dispersion parameter D = 17 ps/nm·km [18]. Note that the quantization noise of analog-to-digital converters (ADCs) is not considered in the present simulations. It is therefore expected that no penalty should be obtained after imbalance compensation and equalization in these simulations, as pointed out in [12].

Fig. 7 presents the BER calculated as a function of the optical signal to noise ratio (OSNR). The OSNR is defined as the ratio between the average optical signal power and the amplified spontaneous emission (ASE) noise power in a reference bandwidth (0.1 nm in our case). The BER is evaluated over 65000 symbols and the calculation is repeated 10 times with different noise seeds for each OSNR value in order to calculate a BER average value. The BER curves depict the cases without (w/o) and with (w/) IQ imbalance compensation in case 2 (where IQ imbalance and equalization are handled simultaneously) after 1200 km optical fiber transmission. In the presence of such a strong IQ imbalance, the signal cannot be recovered (as depicted by the dashed lines) regardless of the transmission distance if the IQ imbalance is not compensated. With the proposed compensation, the BER curves are brought back to the B2B one with no noticeable penalty, as depicted by the dotted lines. The fact that no penalty is obtained after imbalance compensation, in contrast with the ~4 dB penalty measured in the experimental results (Fig. 6), is due to the absence of quantization noise in the simulations, as already pointed out. It should also be noted that the required ADC resolution is expected to be relatively high as the IQ imbalance is increased [12]. These results confirm the effectiveness of the equalizer in the joint compensation configuration.

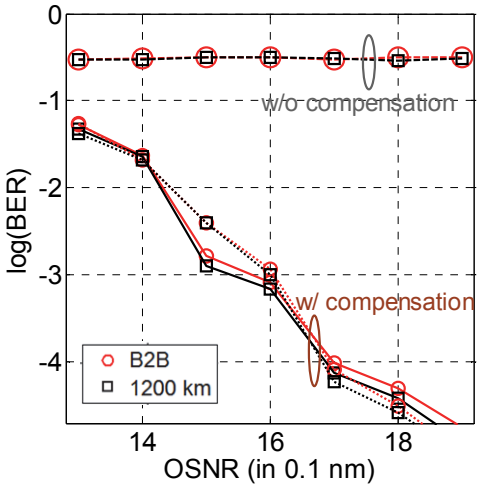

Fig. 7. BER versus OSNR under the impacts of chromatic dispersion and IQ imbalance. Solid lines: no IQ imbalance and with compensation. Dotted lines: with IQ imbalance of 20° and with compensation. Dashed lines: with IQ imbalance of 20° and without compensation.

VII. Conclusion

In this paper, we have proposed and demonstrated a joint blind adaptive equalization method as a promising candidate for in–phase/quadrature imbalance compensation in *m*-QAM systems. The accuracy of this method was experimentally validated by BER evaluations with a 40-Gb/s 16-QAM signal, resulting in 7 dB power penalty reduction at a BER of 10^{-3} for 10° phase imbalance. The effectiveness of the joint method was numerically confirmed with negligible penalty being obtained in the presence of group-velocity dispersion compensation with up to 1200 km optical fiber transmission and 20° phase imbalance.

ACKNOWLEDGEMENT

This work was supported by the French National Research Agency (OCELOT project, ref. ANR-10-VERS-0015), the Contrat de plan Etat-Région Ponant and the French Ministry of Research.

REFERENCES

[1] E. Ip, A. P. T. Lau, D. J. F. Barros, and J. M. Kahn, "Coherent detection in optical fiber systems," Opt. Express, vol. 16, no. 2, pp. 753-791, Jan. 2008.

[2] M. Valkama, M. Renfors, and V. Koivunen, "Advanced methods for I/Q imbalance compensation in communication receivers," IEEE Trans. Signal Process., vol. 49, no. 10, pp. 2335-2344, 2001.

[3] T. C. W. Schenk, P. F. M. Smulders, and E. R. Fledderus, "Estimation and compensation of frequency selective TX/RX IQ imbalance in MIMO OFDM systems," in Proc. IEEE Int. Conf. Commun. (ICC), Helsinki, Finland, pp. 251-256, Jun. 2006.

[4] C.-H. Liu, "Joint Tx and Rx IQ imbalance compensation of OFDM transceiver in mesh network," in Proc. Globel Telecom. Conf. (Globecom'2008), New Orleans, pp. 704-708, Dec. 2008.

[5] W. Chung, "Transmitter IQ mismatch compensation in coherent optical OFDM systems using pilot signals," Opt. Express, vol. 1, no. 20, pp. 21308-21314, 2010.

[6] X. Ma, K. Li, and Y. Bai, "Novel training symbol structure for transmitter IQ mismatch compensation for coherent optical OFDM," IEEE Photon. Technol. Lett., vol. 25, no. 21, pp. 2047-2049, Nov. 2013.

[7] S. Cao, C. Yu, and P. Y. Kam, "Decision-aided joint compensation of transmitter IQ mismatch and phase noise for coherent optical OFDM," IEEE Photon. Technol. Lett., vol. 24, no. 12, pp. 1066-1068, Jun. 2012.

[8] I. Fatadin, S. J. Savory, and D. Ives, "Compensation of quadrature imbalance in an optical QPSK coherent receiver," IEEE Photon. Technol. Lett., vol. 20, no. 20, pp. 1733-1735, Oct. 2008.

[9] S. H. Chang, H. S. Chung, and K. Kim, "Impact of quadrature imbalance in optical coherent QPSK receiver," IEEE Photon. Technol. Lett., vol. 21, no. 11, pp. 709-711, May 2009.

[10] C. S. Petrou, A. Vgenis, I. Roudas, and L. Raptis, "Quadrature imbalance compensation for PDM QPSK coherent optical systems," IEEE Photon. Technol. Lett., vol. 21, no. 24, pp. 1876-1878, Dec. 2009.

[11] Y. Qiao, Y. Xu, L. Li, and Y. Ji, "Quadrature imbalance compensation algorithm based on statistical properties of signals in CO-QPSK system," Chinese Opt. Lett., vol. 10, article no. 120601, pp. 1-4, Oct. 2012.

[12] M. S. Faruk, and K. Kikuchi, "Compensation for In-phase/ Quadrature imbalance in coherent-receiver front-end for optical quadrature amplitude modulation," IEEE Photon. J., vol. 5, no. 2, article no. 7800110, Apr. 2013.

[13] C. Rottondi, M. Tornatore, A. Pattavina, and G. Gavioli, "Routing, modulation level, and spectrum assignment in optical metro ring networks using elastic transceivers," J. Opt. Commun. Netw., vol. 5, no. 4, pp. 305-315, Apr. 2013.

[14] F. M. Gardner, *Phase Lock Techniques*, 2nd edition, John-Wiley & Sons, New York 1979.

[15] J. K. Cavers and M. W. Liao, "Adaptive compensation for imbalance and offset losses in direct conversion transceivers," IEEE Trans. Veh. Technol., vol. 42, no. 4, pp. 581-588, Nov. 1993.

[16] W. Nam, H. Roh, J. Lee, and I. Kang, "Blind adaptive I/Q imbalance compensation algorithms for direct-conversion receivers," IEEE Signal Process. Lett., vol. 19, no. 8, pp. 475-478, Aug. 2012.

[17] I. Fatadin, D. Ives, and S. J. Savory, "Compensation of frequency offset for differentially encoded 16- and 64-QAM in the presence of laser phase noise," IEEE Photon. Technol. Lett., vol. 22, no. 3, pp. 176-178, Feb. 2010.

[18] *Characteristics of single-mode optical fibre and cable,* International Telecommunications Union ITU-T Recommendation G.652, Mar. 2003.